Acta Biomaterialia 7 (2011) 75–82

Contents lists available at ScienceDirect

Acta Biomaterialia

journal homepage: www.elsevier.com/locate/actabiomat

Mitral valvular interstitial cell responses to substrate stiffness depend on age and anatomic region

Elizabeth H. Stephens, Christopher A. Durst, Jennifer L. West, K. Jane Grande-Allen *

Department of Bioengineering, Rice University, P.O. Box 1892 - MS142, Houston, TX 77251-1892, USA

ARTICLE INFO

Article history:
Received 6 May 2010
Received in revised form 1 July 2010
Accepted 2 July 2010
Available online 17 July 2010

Keywords:
Heart valve
Age/aging
Stiffness
Hydrogel
Surface modification

ABSTRACT

The material properties of heart valves depend on the subject's age, the state of the disease and the complex valvular microarchitecture. Furthermore, valvular interstitial cells (VICs) are mechanosensitive, and their synthesis of extracellular matrix not only determines the valve's material properties but also provides an adhesive substrate for VICs. However, the interrelationship between substrate stiffness and VIC phenotype and synthetic properties is poorly understood. Given that the local mechanical environment (substrate stiffness) surrounding VICs differs among different age groups and different anatomic regions of the valve, it was hypothesized that there may be an age- and valve-region-specific response of VICs to substrate stiffness. Therefore, 6-week-, 6-month- and 6-year-old porcine VICs from the center of the mitral valve anterior leaflet (MVAC) and posterior leaflet (PML) were seeded onto poly(ethylene) glycol hydrogels of different stiffnesses and stained for markers of VIC activation (smooth muscle alpha-actin (SMaA)) and collagen synthesis (heat shock protein-47 (HSP47), prolyl 4-hydroxylase (P4H)). Six-week-old MVAC demonstrated decreased SMaA, P4H and HSP47 on stiffer gels, while 6-week-old PML only demonstrated decreased HSP47. Six-month-old MVAC demonstrated no difference between substrates, while 6-month-old PML demonstrated decreased SMaA, P4H and HSP47. Six-year-old MVAC demonstrated decreased P4H and HSP47, while 6-year-old PML demonstrated decreased P4H and increased HSP47. In conclusion, the age-specific and valve-region-specific responses of VICs to substrate stiffness link VIC phenotype to the leaflet regional matrix in which the VICs reside. These data provide further rationale for investigating the role of substrate stiffness in VIC remodeling within diseased and tissue engineered valves.

1. Introduction

Valve disease afflicts a substantial portion of the population: 1–2% of 26- to 84-year-olds are afflicted by mitral valve disorders [1]. Valve disease incurs significant morbidity and mortality, requiring over 100,000 surgeries in the USA each year [2]. In many of these disease states the mechanical properties of these valves are altered, often contributing to the poor valve function requiring surgical intervention. Valvular interstitial cells (VICs) are the dynamic, living component of heart valves responsible for synthesizing and maintaining the valve matrix composition, which in turn determines the valve's material behavior. VICs and valves are known to be responsive to changes in their mechanical environment [3–5]. However, the interplay between matrix-driven material properties such as stiffness and the phenotype and synthetic behavior of VICs, particularly in the mitral valve (MV), has largely been overlooked. Recent work has demonstrated age-related significant changes in valve composition [6–8] and material properties [9]; other studies have shown substantial heterogeneity in material behavior among the different anatomic regions of the MV [10]. Given that different aged VICs and VICs from different regions of the MV reside in valve tissues with distinct stiffnesses [9], it was hypothesized that there may be an age- and valve-region-specific response of VICs to substrate stiffness.

In order to test this hypothesis, separate groups of VICs from three distinct age groups and from two different regions of the MV were cultured on poly(ethylene) glycol (PEG) hydrogels of two different stiffnesses. After 48 h, the resulting VIC expression of cell phenotype and collagen synthesis markers was assessed using immunocytochemistry (ICC).

PEG hydrogels were chosen for this experiment based on their promise as a potential platform for the design of scaffolds for tissue-engineered heart valves. PEG hydrogels are extremely hydrophilic, providing prevention against protein adsorption, a critical step in the immunogenicity and degradation of bioprosthetics [11]. They are also highly permeable, allowing the exchange of nutrients and waste materials [12]. Their stiffness can be regulated by changing the molecular weight and concentration of PEG [13]. However, one of the factors that makes these gels particularly

* Corresponding author. Tel.: +1 713 348 3704; fax: +1 713 348 5877.
E-mail address: grande@rice.edu (K.J. Grande-Allen).

1742-7061/$ - see front matter © 2010 Acta Materialia Inc. Published by Elsevier Ltd. All rights reserved.
doi:10.1016/j.actbio.2010.07.001

attractive is the ability to customize them by conjugating to the PEG backbone various peptides, including cell ligands and growth factors, as well as incorporating enzyme-degradable sequences allowing tunability of the degradation rate of the hydrogel. This designer biofunctionality makes PEG hydrogels advantageous for the tissue engineering of heart valves. In the present study PEG hydrogels were conjugated with an Arg–Gly–Asp–Ser (RGDS) peptide, enabling VIC attachment to the hydrogel, and methacrylated heparin, which is necessary for normal VIC morphology [14,15]. These functionalized PEG hydrogels of two different stiffnesses were formulated to keep the concentration of biological cues constant, thus isolating the effect of stiffness on VIC phenotype.

2. Materials and methods

2.1. Synthesis of PEG hydrogel components

PEG-diacrylate (PEG-DA) of 3400 Da MW was synthesized from PEG (Sigma–Aldrich, St. Louis, MO) as previously described [13]. ^{1}H nuclear magnetic resonance (NMR) analysis revealed >95% acrylation. Methacrylated heparin was synthesized as described previously [14]. Briefly, a 10 mg ml^{-1} solution of heparin (Sigma–Aldrich) dissolved in ultrapure water was reacted with 40 molar excess methacrylic anhydride (Sigma–Aldrich). The pH of the solution was adjusted to 7.5 using 4 M NaOH and stirred for 24 h. Methacrylated heparin was then precipitated using cold 95% ethanol. The precipitate was then filtered, dried and dialyzed against ultrapure water using a 1000 Da MWCO membrane (Spectrum Laboratories, Rancho Dominguez, CA). The product was then lyophilized. ^{1}H NMR analysis revealed 5% methacrylation per disaccharide.

The RGDS peptide (Bachem, Bubendorf, Switzerland) was attached to hetero-bifunctional PEG (PEG-SCM; Laysan Bio, Arab, AL) by reacting the peptide with hetero-bifunctional PEG and catalyst diisopropylamine (Sigma–Aldrich) in dimethyl sulfoxide (DMSO; 1.2 M RGDS:1.0 M PEG-SCM:2.0 M disopropylamine) for 24 h. The product was then dialyzed against ultrapure water using a 1000 Da MWCO membrane (Spectrum Laboratories) and lyophilized. The Trp–Arg–Gly–Asp–Ser (WRGDS) peptide (GenScript, Piscataway, NJ) was similarly attached to hetero-bifunctional PEG. Evaluation of PEG-RGDS by gel permeation chromatography revealed 81% conjugation.

2.2. Polymerization of functionalized PEG hydrogels

PEG hydrogels were synthesized by dissolving the appropriate amounts of PEG-RGDS, methacrylated heparin and PEG-DA in phosphate-buffered saline. A volume of 10 μl ml^{-1} 2,2-dimethoxy-2-phenyl-acetophenone (300 mg ml^{-1} in 1-vinyl-2-pyrrolidone) was added and the solution was poured between two sterile glass slides separated by a 0.4 mm spacer and exposed to ultraviolet light for 2 min (365 nm, 10 mW cm^{-2}). Hydrogels were then removed from the mold and soaked in phosphate-buffered saline with 2% antibiotic (Mediatech, Herndon, VA) for at least 24 h allowing the hydrogels to swell to equilibrium. Hydrogel thickness was optically measured using a Leica DFC 320 CCD camera (Wetzlar, Germany) and ImagePro acquisition software (Media Cybernetics, Bethesda, MD). Hydrogel thicknesses were determined from the acquired images using ImageJ software (NIH, Bethesda, MD).

2.3. Optimization of functionalized PEG hydrogels

Optimization studies were performed to determine the concentrations of PEG-RGDS and methacrylated heparin in the pre-polymer solution necessary to yield equivalent amounts of these bioactive ligands in the swollen, polymerized gels of the two different weight–volume fractions of PEG-DA. The concentration of methacrylated heparin in polymerized, swollen gels was determined using an uronic acid assay, as described by Blumenkrantz and Asboe-Hansen [16] after gels were hydrolyzed by reacting them with 0.1 N NaOH for 34 h at 37 °C. These studies determined that 9.0 mg ml^{-1} of methacrylated heparin in the pre-polymer hydrogel solution for the 5% weight–volume PEG-DA hydrogel and 10.6 mg ml^{-1} of methacrylated heparin in the solution for the 15% weight–volume PEG-DA hydrogel yielded equivalent concentrations of methacrylated heparin in the polymerized, swollen gels of the different PEG-DA weight–volume fractions (Fig. 1). Optimization studies utilizing tryptophan (which was detected by its absorbance at 280 nm using a spectrophotometer (SpectraMax M2, Molecular Devices, Sunnyavale, CA)) in the RGDS peptide (WRGDS, conjugated to PEG using the same reaction as for RGDS; gel permeation chromatography revealed 83% conjugation), determined that 7.49 mg ml^{-1} of PEG-RGDS in the pre-polymer solutions for both weight–volume PEG-DA hydrogels yielded equivalent final concentrations of PEG-RGDS in the swollen, polymerized gels (Fig. 2).

2.4. Determination of elastic modulus of functionalized PEG hydrogels

Strips of the two weight–volume fraction PEG hydrogels (5 mm in width) were uniaxially tensile tested using an EnduraTec ELF 3200 (Bose, Eden Prairie, MN). The strain rate was 10 mm s^{-1} and load–elongation data were recorded until failure occurred. Displacement was converted to strain based on the initial hydrogel length between grips. The elastic modulus was determined as the slope of the least-squares linear fit to the stress–strain curve.

2.5. Cell culture and cell seeding onto PEG

Mitral valves were dissected from hearts from 6-week-, 6-month- and 6-year-old pigs obtained from an abattoir (the 6-week- and 6-month-olds from Fisher Ham and Meat, Spring, TX; the 6-year old from Animal Technologies, Tyler, TX). Based on previous studies demonstrating that the mitral valve anterior center (MVAC) is stiffer than the posterior leaflet [10], VICs were isolated from the MVAC (representing a stiffer valve region) and the PML (representing a less stiff valve region) from the same mitral valves according to previously published protocols [17]; cells were cultured in medium containing 10% bovine growth serum (HyClone, Logan, UT) and 2% antibiotic/antimycotic (Mediatech). The medium was changed every 2–3 days and cells were passaged after reaching

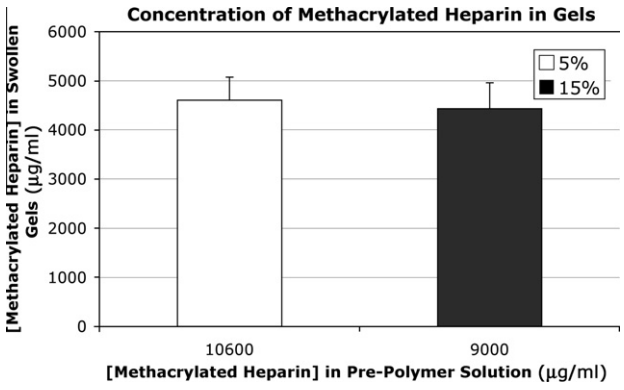

Fig. 1. Concentration of methacrylated heparin in the two different weight–volume fraction PEG swollen gels as determined by uronic acid assay. Four PEG hydrogel samples of each weight–volume fraction were tested. Error bars on all graphs indicate standard error of the mean.

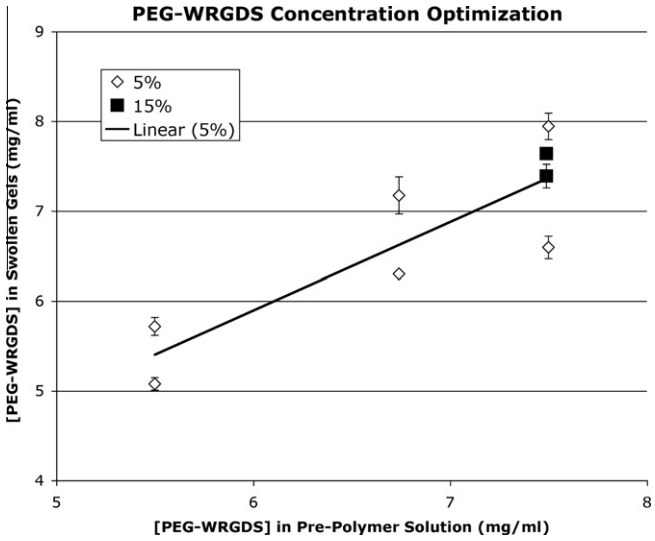

Fig. 2. Optimization of PEG-WRGDS in the two different weight–volume fraction PEG swollen gels by varying the concentration of PEG-WRGDS in the pre-polymer solutions. The concentration of PEG-WRGDS was determined by absorption at 280 nm.

80–90% confluence. Experiments were performed on cells from passages 5–6. Cells were seeded onto functionalized PEG hydrogels at a cell density of 6000 cells cm^{-2} and maintained in 10% serum medium with 2% antibiotic/antimycotic.

2.6. Immunocytochemistry

Based on previous reports demonstrating phenotypic changes in fibroblasts and VICs after 24–48 h [14,18], in the present study VICs were cultured on gels for 48 h and then fixed by incubation in 10% formaldehyde in PBS for 30 min at room temperature. Samples of dimensions 4 mm × 6 mm were cut from cell-seeded gels and transferred to the wells of an 8-well coverglass chamber (Lab-Tek II, Nalge Nunc International, Naperville, IL) for ICC staining and subsequent imaging. ICC was performed for markers of collagen synthesis prolyl 4-hydroxylase (P4H; Chemicon, Temecula, CA) and heat shock protein 47 (HSP47; Assay Designs, Ann Arbor, MI), as well as markers related to valve cell phenotype vimentin (Dakocytomation, Denmark) and the marker of VIC activation [19] smooth muscle alpha-actin (SMaA; Dakocytomation), with AlexaFluor 488 secondary antibodies (Invitrogen Molecular Probes, Eugene, OR). Stained gels were imaged using LSM 5 LIVE 5 DuoScan (Zeiss, Oberkochen, Germany) and staining intensity and cell morphology (area and circularity) were quantified using ImageJ software. For determination of staining intensity, cells were outlined and the intensity within each cell was quantified (0–255) relative to any background intensity. Multiple images (3–5) were analyzed for each marker for each VIC population cultured on the different gels.

2.7. Statistical analysis

Multifactorial analysis of variance (ANOVA) was performed using SigmaStat (SPSS, Chicago, IL). When the data for a given characteristic was normally distributed (as determined by the software), the program continued with an ANOVA. When the data set was not normally distributed, the data was rank transformed before the ANOVA was performed. In both cases the level of significance was set at 0.05.

3. Results

3.1. Stiffness of different weight–volume fraction functionalized PEG hydrogels

Uniaxial testing revealed that functionalized 5% weight–volume PEG gels had a mean modulus of 34.5 kPa, while functionalized 15% weight–volume PEG gels had a mean modulus of 323.3 kPa (Fig. 3).

3.2. SMaA expression of VICs on gels of different stiffnesses

Not all VICs stained positively for SMaA, as expected. Analysis of the fraction of VICs expressing SMaA (SMaA+ VICs) on the different gels revealed a trend towards decreased SMaA+ VICs on the 15% gels compared to the 5% in the 6-week-old MVAC VICs (Fig. 4, $p = 0.1$), but there was no difference between gels for 6-week-old PML VICs. Six-month- and 6-year-old MVAC VICs did not display a difference in the fraction of SMaA+ VICs between gels, but 6-month- and 6-year-old PML VICs showed a trend toward decreased SMaA + VICs on the 15% gels relative to the 5% gels ($p = 0.06$). Analysis of the intensity of SMaA stain in SMaA+ VICs on the different gels revealed a trend towards decreased intensity in SMaA+ VICs for 6-week-old MVAC VICs (Fig. 5, $p = 0.087$) but no difference for 6-week-old PML VICs. Six-month-old MVAC demonstrated no change in SMaA intensity in MVAC VICs but decreased SMaA intensity in PML VICs ($p < 0.05$). No difference in SMaA intensity between gels was evident for 6-year-old MVAC VICs or 6-year-old PML VICs.

3.3. P4H expression of VICs on gels of different stiffnesses

Analysis of P4H, which was expressed by all VICs, demonstrated decreased intensity in 6-week-old MVAC VICs on the 15% gels relative to the 5% gels ($p < 0.05$) but no difference between gels for 6-week-old PML VICs. Six-month-old MVAC VICs demonstrated no difference in P4H intensity between gels, but 6-month-old PML VICs demonstrated decreased intensity on the 15% gels relative to the 5% gels (Fig. 6, $p < 0.05$). Six-year-old MVAC and PML VICs both demonstrated decreased P4H intensity on the 15% gels relative to the 5% gels (MVAC $p < 0.05$, PML $p < 0.085$ (trend)).

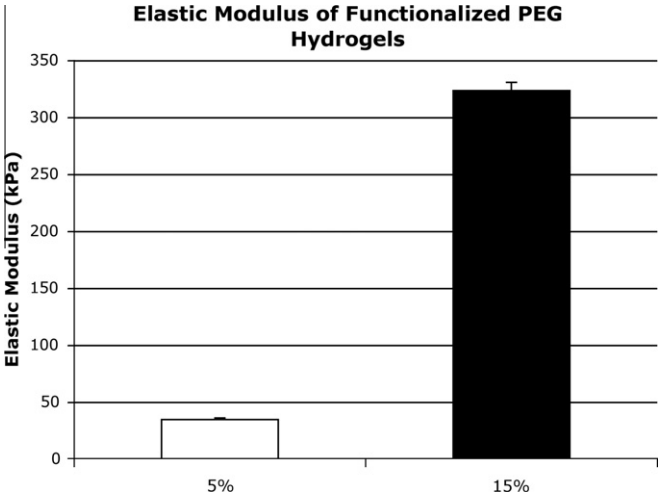

Fig. 3. Stiffness of the two weight–volume fraction functionalized PEG gels as determined by the elastic modulus during uniaxial tensile testing. Four PEG hydrogel samples of each weight–volume fraction were tested.

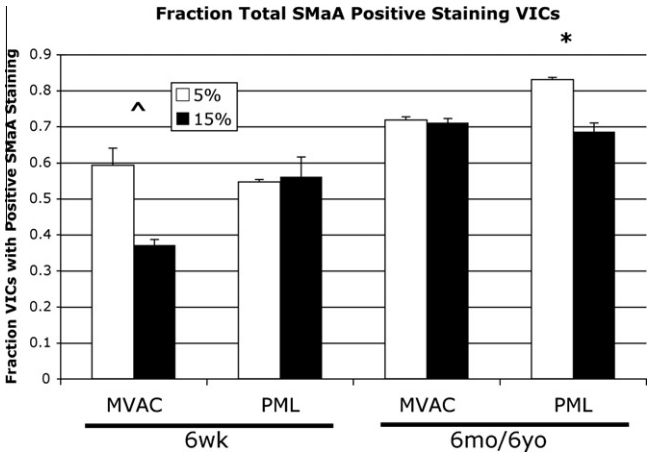

Fig. 4. Percent VICs displaying positive SMaA staining on the two gels of different stiffnesses, $^{*}p = 0.06$, $^{\wedge}p = 0.1$ 5% vs. 15% gels. Data from the 6-month-old and 6-year-old age groups were not significantly different and so were grouped together; the combined data are shown.

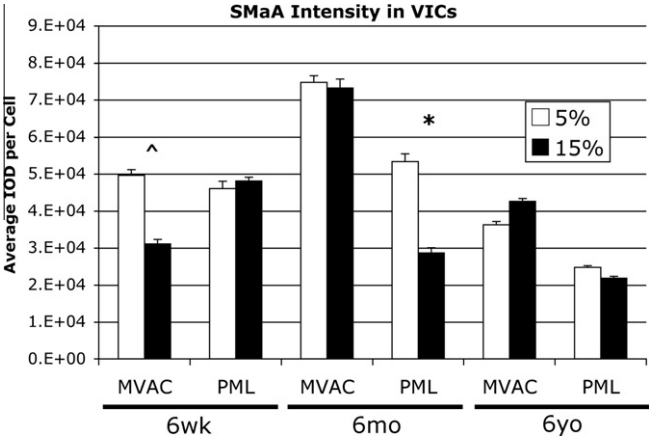

Fig. 5. SMaA staining intensity for positive SMaA staining VICs on the two gels of different stiffnesses. $^{*}p < 0.05$, $^{\wedge}p = 0.087$ 5% vs. 15% gels.

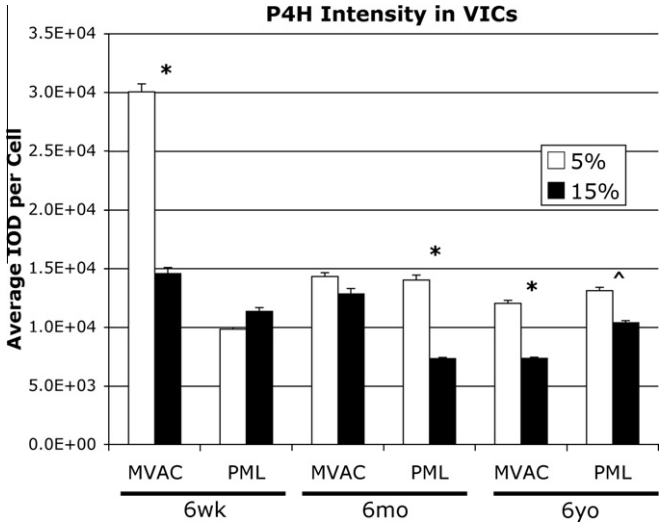

Fig. 6. P4H staining intensity of VICs on the two gels of different stiffnesses. $^{*}p < 0.05$, $^{\wedge}p < 0.085$ 5% vs. 15% gels.

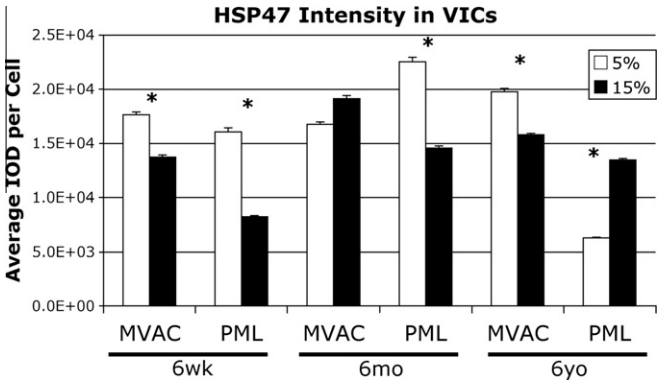

Fig. 7. HSP47 staining intensity of VICs on the two gels of different stiffnesses. $^{*}p < 0.05$ 5% vs. 15% gels.

3.4. HSP47 expression of VICs on gels of different stiffnesses

Analysis of HSP47, which was expressed by all VICs, demonstrated decreased intensity in both 6-week-old MVAC and PML VICs on the 15% gels relative to the 5% gels (Fig. 7, both $p < 0.05$). Six-month-old MVAC VICs demonstrated no difference in HSP47 intensity between gels, but 6-month-old PML VICs demonstrated decreased HSP47 intensity on the 15% gels relative to the 5% gels ($p < 0.05$). Six-year-old MVAC demonstrated no difference in HSP47 intensity between gels, but 6-year-old PML VICs demonstrated increased HSP47 intensity on the 15% gels relative to the 5% gels ($p < 0.05$).

3.5. VIC Morphology on gels of different stiffnesses

For both MVAC and PML VICs of each age and on each gel, two populations of VICs were noted: one with a spindle-shaped cell morphology and a second with a cuboidal cell morphology (Fig. 8). Analysis of staining intensity of cuboidal and spindle-shaped subpopulations revealed that, for given age- and valve-region VICs that responded to substrate stiffness, both subpopulations demonstrated a response (data not shown). Cell morphology analysis of vimentin-stained VICs revealed a decreased cell area of 6-month-old PML VICs on the 15% gels relative to the 5% gels ($p < 0.02$). No difference was noted in circularity between VICs on PEG hydrogels of different stiffnesses.

4. Discussion

In this study, mitral VICs grown on functionalized PEG hydrogels demonstrated both age- and valve-region-specific (MVAC vs. PML) responses to substrate stiffness. These results underscore the range of unique phenotypes found in valvular cells and provide compelling motivation for further studies of heart valve mechanobiology.

4.1. Previous studies of VICs and substrate stiffness

While the response of cells to substrate stiffness has been studied extensively in cell types from many other tissues (see the excellent review by Nemir and West [20]), very limited investigation has been performed on the response of VICs to substrate stiffness. Furthermore, even though the material properties of MVs are known to be altered in diseased states [21,22] and are distinct in different MV regions [10], no studies published to date have examined the response of MV VICs to substrate stiffness. Additionally, no studies have investigated a potential age-specific response of VICs to substrate stiffness despite a growing awareness that valve

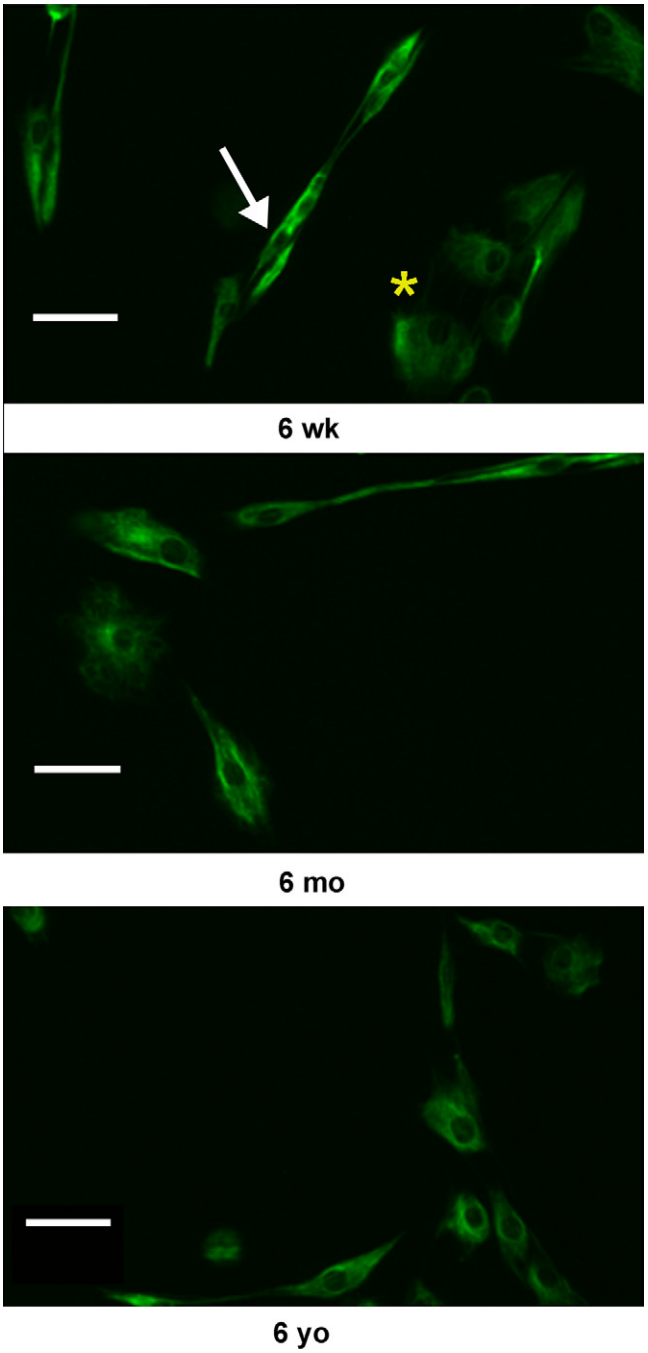

Fig. 8. Images of vimentin-stained VICs from each age group demonstrating two distinct VIC morphologic subpopulations: spindle-shaped cells (see the white arrow in the 6-week-old image) and cuboidal cells (see the yellow asterisk in the 6-week-old image). These distinct subpopulations were evident for VICs isolated from both MVAC and PML and on PEG gels of both stiffnesses. Shown here are MVAC VICs on 15% PEG gels. Scale bars indicate 50 mm.

matrix, material properties and VIC phenotype change with age [6–9].

Work on fibroblasts from different tissues examining cell phenotype and morphology changes in response to substrate stiffness has documented increased actin fibers in response to increased substrate stiffness [20], appearance of stress fibers on stiffnesses of 10 kPa and above [18], and an increase in cell spreading that was maximum on substrate stiffnesses of 8–10 kPa [18,23]. However, all of these studies were performed within a range of substrate stiffnesses that was much lower (i.e. 1–100 kPa [20]) than the stiffnesses used in the present study. While the in vivo stiffness of the MVAC continues to be debated [24,25], and the in vivo stiffness of the PML remains to be determined, these stiffnesses are certainly considerably greater than the 1–10 kPa range of substrate stiffness commonly utilized in fibroblast experiments. The two gel stiffnesses used in this study were chosen to be in the same general range that could be consistent with the in vivo stiffnesses of the MVAC and PML, yet were different enough to potentially elicit age- and valve-region-specific VIC responses.

Three previous studies aimed at identifying factors in aortic valve (AV) calcification have analyzed the effect of substrate stiffness on mineralization and activation of porcine AV VICs. One work [26] compared the calcification potential of AV VICs seeded at confluence (allowing cell-to-cell interaction) on PEG hydrogels (compressive modulus of ~100 kPa) functionalized with fibronectin or fibrin to AV VICs cultured on unmodified tissue culture polystyrene (TCPS, a much stiffer substrate) and TCPS coated with fibrin and fibronectin [26]. One of their key findings was that the response of VICs to substrate stiffness depended on the matrix coating the substrate [26]. Another study showed that porcine AV VICs cultured on collagen gels of different stiffnesses did not display any difference in calcification potential in normal medium, but in calcification medium AV VICs developed different types of calcific nodules depending on the collagen gel stiffness [27]. In an earlier study [28], SMaA expression in AV VICs was increased on stiffer collagen gels; however, in this study VICs were simultaneously exposed to different concentrations of collagen fibers and this may have confounded the interpretation of their results [28].

4.2. Age- and valve-region-specific responses of VICs to substrate stiffness

In the present study both age- and valve-region-specific responses of VICs to different substrate stiffnesses were evident. Based on ex vivo experiments of material properties of different aged porcine MVs and different regions within the porcine MV (MVAC vs. PML [10]), one would expect the 6-week-old VICs to be accustomed to a less stiff substrate relative to the 6-month- and 6-year-old VICs. Similarly, given studies demonstrating that MVAC tissues are stiffer than PML tissues [10], one would expect MVAC VICs to be accustomed to a stiffer substrate than PML VICs. Unfortunately, the actual in vivo stiffness of the MVAC remains unclear, with only a few reports citing vastly differing values [24,25]; no reports exist citing values for the in vivo stiffnesses of different aged MVAC and PML. Potentially, the results from this study could be explained by differences in "optimal" stiffness for each VIC population assessed. Just as "optimal" stiffnesses have been demonstrated for stem cell lineage specification and the expression of associated cellular markers [29], in VICs expression of myofibroblast phenotype and collagen synthesis markers may reach a maximum at a certain stiffness, and this stiffness could be unique for each VIC population. Based on the mechanical testing studies cited above, potentially the "optimal" stiffness for 6-week-old PML would be less than those for 6-month-old PML and 6-week-old MVAC. Where the stiffnesses of the 5% and 15% gels fall relative to one another upon this hypothetical marker expression–stiffness curve for a particular VIC population could explain whether differences in marker expression were observed between the VIC population seeded on the 5% and 15% gels (Fig. 9). Clearly, substantial future work is needed to investigate this hypothesis further, including a larger number and range of substrate stiffnesses. Nevertheless, the results from this study demonstrate that there are age- and valve-region-specific responses of VICs to substrate stiffness.

In terms of specific protein expression, SMaA expression and proportion of SMaA+ cells generally paralleled changes in collagen

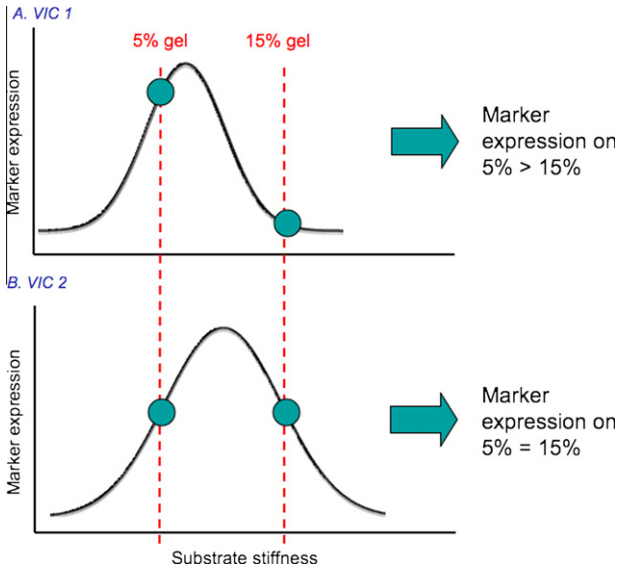

Fig. 9. Schematic illustrating how differences or lack of differences in marker expression between 5% and 15% gels may relate to a hypothetical marker expression–substrate stiffness continuum that is distinct for each VIC population (i.e. age and valve region). The stiffnesses of the 5% and 15% gels fall on the marker expression–substrate stiffness curve in A such that marker expression on 5% gels is greater than on 15% gels, whereas the 5% and 15% gels fall on the marker expression–substrate stiffness curve in B such that marker expression on the 5% gels and 15% gels are equal.

synthesis markers in 6-week-old and 6-month-old MVAC and PML VICs. However, in 6-year-old VICs changes were evident in markers of collagen synthesis despite no detectable change in SMaA intensity. Benton et al. [26] similarly found some uncoupling between stiffness-mediated changes in SMaA expression and calcification potential of AV VICs. While the results for HSP47 largely paralleled those of P4H, in 6-year-old PML VICs P4H expression was decreased on 15% gels relative to 5% gels, while HSP47 was increased. Other studies, however, confirm the potential for independent regulation of HSP47 and other markers of collagen synthesis (such as P4H) by mechanically stressed tendon cells [30] and fibroblasts treated with transforming growth factor-beta [31]. Certain enzymes, such as lysyl hydroxylase 2, have also demonstrated differential regulation of HSP47 and P4H in dermal fibroblasts [32]. Therefore, it appears reasonable for HSP47 to show distinct changes in response to substrate stiffness relative to P4H.

As anticipated, based on inherent differences between VICs from AV compared to MV [33,34], the SMaA results in this study are different from those of AV VICs reported by Pho et al. [28]. Additional distinctions between these two studies, such as cell seeding density, different adhesive substrates and range of substrate stiffnesses [28], may also have contributed to the different results. Work by Engler et al. [29] has demonstrated that for stem cells there exists a stiffness at which there is a maximum in myofibroblast marker expression, and above this stiffness myofibroblast marker expression actually decreases, which would be consistent with the findings of this study. Differences in the results between the Pho et al. study [28] and the present study may also be due to the matrix components used in the substrates of different stiffnesses.

4.3. VIC subpopulations

Distinct VIC subpopulations, including the spindle-shaped and cuboidal cell morphologies evident in this study, have been previously documented [35,36]. The spindle-shaped cells demonstrate qualities similar to fibroblasts, while those with cuboidal morphology are similar to myofibroblasts and are associated with valve remodeling and various valve pathologies [19,35–37]. These subpopulations also demonstrate differences in adhesion to different substrates and matrix components, such as fibronectin [38,39]. In the present study, when a difference in marker expression in VICs between the gels of different stiffnesses was evident, both subpopulations appeared to display this difference. Recent advances in the isolation of these subpopulations could allow a more in-depth investigation of these subpopulations with respect to substrate stiffness [39].

4.4. Implications

These distinct responses of VICs from different-aged MVs and different MV regions have important implications for our understanding of valve mechanobiology and motivate further study in the context of various diseased states. In light of the fact that these different VIC populations (from different aged valves and from different regions) reside in matrices of different stiffnesses, these results suggest that the in vivo mechanical environment in which VICs reside has a profound, fundamental impact on the responsiveness of VICs to their external environment (i.e. their baseline intracellular signaling framework), even in the ex vivo setting. In the context of normal aging, these distinct responses could relate to the ability of the valve to remodel appropriately in response to age-related changes in hemodynamics. With respect to normal physiology, the region-specific differences may relate to the different loading patterns that these regions experience. The age-specific differences could relate to the predilection of certain valve diseases to occur at certain ages, and the valve-region-specific responses could relate to the propensity of certain valve diseases to preferentially affect specific regions of the MV. Knowledge of cell–substrate interactions also has relevance for valve tissue engineering; the design of a tissue-engineered heart valve scaffold should consider how its stiffness affects the phenotype and matrix synthesis of whatever cells will be seeded within or recruited into the scaffold. The results from this study suggest that the scaffold stiffness may need to be carefully tuned depending on the cell type used.

4.5. Limitations and future studies

While the results of this study provide fundamental knowledge regarding how MV VICs respond to substrate stiffness, substantial work still needs to be done in this area and certain study limitations should be noted. While the concentrations of biological cues presented to these cells (RGDS and methacrylated heparin) were carefully orchestrated to be the same between the two substrates, there may be differences in how different aged VICs and VICs from different valve regions respond to the same concentration of these biological cues (for example, if cultured on tissue culture plastic). Future studies investigating this further, examining how these short-term changes relate to longer term changes and downstream processes, and perhaps assessing differences in how these cells interact with their substrate (i.e. expression of integrins), would add insight in this area. Additionally, the mechanism(s) by which these cells respond differently to their substrate warrants investigation. For instance, while PEG is highly hydrophilic and does not adsorb proteins, heparin is known to bind growth factors [40]. Therefore, differences in the amounts or types of growth factors produced by these different VICs in response to different substrates could then be sequestered by heparin in the gels and propagate changes in the VIC phenotype. Future investigation into inherent differences between these VIC populations could also lend insight into the results found in this study. Ultimately, a larger range of substrate stiffnesses, including stiffnesses that match those in

which these different VICs reside in vivo, could allow the determination of an "optimal" substrate stiffness for each VIC population. However, this has been difficult given the limited, conflicting reports regarding the in vivo stiffnesses of the MVAC [24,25] and the lack of any in vivo studies of the PML. The goal of this set of experiments was to first determine whether there were age- and valve-region-specific responses to substrate stiffness. An exciting topic for future studies is the role of substrate stiffness in the pathogenesis of mitral valve diseases, such as myxomatous degeneration, and how age-specific and region-specific responses of VICs to substrate stiffness might relate to the incidence of myxomatous changes in particular age groups and valve regions. It should be noted that the time point of 48 h was chosen as it allowed sufficient time for cell adhesion, interaction with the matrix and phenotypic changes, while being short enough so as to not be confounded by potential differences in cell proliferation between the different VIC populations. However, it will be important in the future to examine how these short-term changes relate to downstream processes and longer term changes.

5. Conclusions

In this study, the response of MV VICs to substrate stiffness has been investigated for the first time. VIC populations taken from different regions of the same MV and VICs of different ages cultured on PEG hydrogels of different stiffnesses demonstrated age- and valve-region-specific responses to substrate stiffness. These findings should be taken into consideration in the design of an age-specific tissue-engineered heart valve and in future investigations of heart valve mechanobiology.

Acknowledgements

The authors appreciate the assistance of the members of the Grande-Allen laboratory, as well as members of the West laboratory: Michael Cuchiara, Stephanie Nemir, Ph.D., Melissa McHale, Ph.D., Maude Rowland, Jean Altus, Ph.D. and Jerome Saltarelli, Ph.D. The authors also appreciate the counsel of Scott Baggett, Ph.D. regarding statistics and the assistance of Sean Moran, Ph.D. in NMR analysis. This research was supported in part by a Hertz Foundation Graduate Fellowship (E.H.S.), a NIH Ruth Kirschstein (F30) National Research Service Award (E.H.S), and a grant from the March of Dimes (J.G.A).

Appendix A. Figures with essential colour discrimination

Certain figures in this article, particularly Figures 8 and 9, are difficult to interpret in black and white. The full colour images can be found in the on-line version, at 10.1016/j.actbio.2010.07.001.

References

[1] Rosamond W, Flegal K, Friday G, Furie K, Go A, Greenlund K, et al. Heart disease and stroke statistics – 2007 update: a report from the American Heart Association Statistics Committee and Stroke Statistics Subcommittee. Circulation 2007;115:e69–171.
[2] American Heart Association. Heart disease and stroke statistics – 2008 update. Dallas, TX, 2008.
[3] Ku CH, Johnson PH, Batten P, Sarathchandra P, Chambers RC, Taylor PM, et al. Collagen synthesis by mesenchymal stem cells and aortic valve interstitial cells in response to mechanical stretch. Cardiovasc Res 2006;71:548–56.
[4] Balachandran K, Konduri S, Sucosky P, Jo H, Yoganathan AP. An ex vivo study of the biological properties of porcine aortic valves in response to circumferential cyclic stretch. Ann Biomed Eng 2006;34:1655–65.
[5] Platt MO, Xing Y, Jo H, Yoganathan AP. Cyclic pressure and shear stress regulate matrix metalloproteinases and cathepsin activity in porcine aortic valves. J Heart Valve Dis 2006;15:622–9.
[6] Stephens EH, Chu CK, Grande-Allen KJ. Valve proteoglycan content and glycosaminoglycan fine structure are unique to microstructure mechanical load and age: relevance to an age-specific tissue-engineered heart valve. Acta Biomater 2008;4:1148–60.
[7] Stephens EH, Grande-Allen KJ. Age-related changes in collagen synthesis and turnover in porcine heart valves. J Heart Valve Dis 2007;16:672–82.
[8] Aikawa E, Whittaker P, Farber M, Mendelson K, Padera RF, Aikawa M, et al. Human semilunar cardiac valve remodeling by activated cells from fetus to adult: implications for postnatal adaptation pathology, and tissue engineering. Circulation 2006;113:1344–52.
[9] Stephens EH, De Jonge N, McNeill MP, Durst CA, Grande-Allen KJ. Age-related changes in material behavior of porcine mitral and aortic valves and correlation to matrix composition. Tissue Eng Part A 2010;16:867–78.
[10] Kunzelman KS, Cochran RP. Stress/strain characteristics of porcine mitral valve tissue: parallel versus perpendicular collagen orientation. J Cardiovasc Surg 1992;7:71–8.
[11] Gombotz W, Wang G, Horbett T, Hoffman A. Protein adsorption to poly(ethylene oxide) surfaces. J Biomed Mater Res 1991;25:1547–62.
[12] Zheng S, Liu Y, Palumbom F, Luo Y, Prestwich G. In situ crosslinkable hyaluronan hydrogels for tissue engineering. Biomaterials 2004;25:1339–48.
[13] Hahn M, McHale M, Wang E, Schmedlen R, West J. Physiologic pulsatile flow bioreactor conditioning of poly(ethylene glycol)-based tissue engineered vascular grafts. Ann Biomed Eng 2007;35:190–200.
[14] Cushing MC, Liao J, Jaeggli MP, Anseth KS. Material-based regulation of the myofibroblast phenotype. Biomaterials 2007;28:3378–87.
[15] Masters KS, Shah DN, Walker G, Leinwand LA, Anseth KS. Designing scaffolds for valvular interstitial cells: cell adhesion and function on naturally derived materials. J Biomed Mater Res A 2004;71:172–80.
[16] Blumenkrantz N, Asboe-Hansen G. New method for quantitative determination of uronic acids. Anal Biochem 1973;54:484–9.
[17] Stephens EH, Carroll JL, Grande-Allen KJ. The use of collagenase III for the isolation of porcine aortic valvular interstitial cells: rationale and optimization. J Heart Valve Dis 2007;16:175–83.
[18] Yeung T, Georges PC, Flanagan LA, Marg B, Ortiz M, Funaki M, et al. Effects of substrate stiffness on cell morphology cytoskeletal structure, and adhesion. Cell Motil Cytoskeleton 2005;60:24–34.
[19] Rabkin E, Aikawa M, Stone JR, Fukumoto Y, Libby P, Schoen FJ. Activated interstitial myofibroblasts express catabolic enzymes and mediate matrix remodeling in myxomatous heart valves. Circulation 2001;104:2525–32.
[20] Nemir S, West JL. Synthetic materials in the study of cell response to substrate rigidity. Ann Biomed Eng 2010;38:2–20.
[21] Imanaka K, Takamoto S, Ohtsuka T, Oka T, Furuse A, Omata S. The stiffness of normal and abnormal mitral valves. Ann Thorac Cardiovasc Surg 2007;13:178–84.
[22] Grande-Allen K, Barber J, Klatka K, Houghtaling P, Vesely I, Moravec C, et al. Mitral valve stiffening in end-stage heart failure: evidence of an organic contribution to functional mitral regurgitation. J Thorac Cardiovasc Surg 2005;130:783–90.
[23] Solon J, Levental I, Sengupta K, Georges PC, Janmey PA. Fibroblast adaptation and stiffness matching to soft elastic substrates. Biophys J 2007;93:4453–61.
[24] Krishnamurthy G, Itoh A, Bothe W, Swanson JC, Kuhl E, Karlsson M, et al. Stress–strain behavior of mitral valve leaflets in the beating ovine heart. J Biomech 2009;42:1906–16.
[25] Sacks MS, Enomoto Y, Graybill JR, Merryman WD, Zeeshan A, Yoganathan AP, et al. In-vivo dynamic deformation of the mitral valve anterior leaflet. Ann Thorac Surg 2006;82:1369–77.
[26] Benton JA, Kern HB, Anseth KS. Substrate properties influence calcification in valvular interstitial cell culture. J Heart Valve Dis 2008;17:689–99.
[27] Yip CY, Chen JH, Zhao R, Simmons CA. Calcification by valve interstitial cells is regulated by the stiffness of the extracellular matrix. Arterioscler Thromb Vasc Biol 2009;29:936–42.
[28] Pho M, Lee W, Watt D, Laschinger C, Simmons C, McCulloch C. Cofilin is a marker of myofibroblast differentiation in cells from porcine aortic cardiac valves. Am J Physiol Heart Circ Physiol 2008;294:H1767–1778.
[29] Engler AJ, Sen S, Sweeney HL, Discher DE. Matrix elasticity directs stem cell lineage specification. Cell 2006;126:677–89.
[30] Pan H, Halper J. Regulation of heat shock protein 47 and type I procollagen expression in avian tendon cells. Cell Tissue Res 2003;311:373–82.
[31] Sasaki H, Sato T, Yamauchi N, Okamoto T, Kobayashi D, Iyama S. Et al., Induction of heat shock protein 47 synthesis by TGF-beta and IL-1 beta via enhancement of the heat shock element binding activity of heat shock transcription factor 1. J Immunol 2002;168:5178–83.
[32] Wu J, Reinhardt DP, Batmunkh C, Lindenmaier W, Far RK, Notbohm H, et al. Functional diversity of lysyl hydroxylase 2 in collagen synthesis of human dermal fibroblasts. Exp Cell Res 2006;312:3485–94.
[33] Walker GA, Masters KS, Shah DN, Anseth KS, Leinwand LA. Valvular myofibroblast activation by transforming growth factor-beta: implications for pathological extracellular matrix remodeling in heart valve disease. Circ Res 2004;95:253–60.
[34] Liu AC, Gotlieb AI. Transforming growth factor-beta regulates in vitro heart valve repair by activated valve interstitial cells. Am J Pathol 2008;173:1275–85.
[35] Taylor PM, Batten P, Brand NJ, Thomas PS, Yacoub MH. The cardiac valve interstitial cell. Int J Biochem Cell Biol 2003;35:113–8.
[36] Messier Jr RH, Bass BL, Aly HM, Jones JL, Domkowski PW, Wallace RB, et al. Dual structural and functional phenotypes of the porcine aortic valve interstitial population: characteristics of the leaflet myofibroblast. J Surg Res 1994;57:1–21.

[37] Rabkin-Aikawa E, Farber M, Aikawa M, Schoen FJ. Dynamic and reversible changes of interstitial cell phenotype during remodeling of cardiac valves. J Heart Valve Dis 2004;13:841–7.
[38] Blevins TL, Carroll JL, Raza AM, Grande-Allen KJ. Phenotypic characterization of isolated valvular interstitial cell subpopulations. J Heart Valve Dis 2006;15:815–22.
[39] Stephens EH, Huynh TN, Cieluch JD, Grande-Allen KJ. Fibronectin-based isolation of valve interstitial cell subpopulations: relevance to valve disease. J Biomed Mater Res A 2010;92:340–9.
[40] Cushing MC, Liao JT, Anseth KS. Activation of valvular interstitial cells is mediated by transforming growth factor-beta1 interactions with matrix molecules. Matrix Biol 2005;24:428–37.